Bioorg. Med. Chem. Lett. 45 (2021) 128161

Contents lists available at ScienceDirect

Bioorganic & Medicinal Chemistry Letters

journal homepage: www.elsevier.com/locate/bmcl

Linderapyrone: A Wnt signal inhibitor isolated from *Lindera umbellata*

Takahiro Matsumoto [a,*], Takahiro Kitagawa [a], Daisuke Imahori [a], Atsushi Matsuzaki [a], Youhei Saito [a], Tomoe Ohta [b], Tatsusada Yoshida [b], Yuji Nakayama [a], Eishi Ashihara [a], Tetsushi Watanabe [a,*]

[a] *Kyoto Pharmaceutical University, Misasagi, Yamashina-ku, Kyoto 607-8414, Japan*
[b] *Nagasaki International University, Nagasaki 859-3298, Japan*

ARTICLE INFO

Keywords:
Linderapyrone
Lindera umbellata
Wnt signal
TCF/*β*-catenin transcriptional activity
DNA microarray analysis

ABSTRACT

Linderapyrone, a Wnt signal inhibitor was isolated from the methanolic extract of the stems and twigs of *Lindera umbellata* together with *epi*-(-)-linderol A. Linderapyrone inhibited TCF/*β*-catenin transcriptional activity that was evaluated using cell-based TOPFlash luciferase assay system. To evaluate the structure-activity relationship and mechanism, we synthesized linderapyrone and its derivatives from piperitone. As the results of further bioassay for synthesized compounds, we found both of pyrone and monoterpene moieties were necessary for inhibitory effect. cDNA microarray analysis in a linderapyrone derivative treated human colorectal cancer cells showed that this compound downregulates Wnt signaling pathway. Moreover, we successes to synthesize the derivative of linderapyrone that has stronger inhibitory effect than linderapyrone and ICG-001 (positive control).

The Wnt signaling pathway plays an important role in various cancer cells, including their proliferation and survival via Tcell factor (TCF)/β -catenin transcription. Previous studies have demonstrated the high occurrence of Wnt pathway mutations in various type of cancers including colon cancer.[1,2] In addition, Wnt signaling pathway is essential for the maintenance of cancer stem cells that deeply related to the tumorigenesis, progression, metastasis, recurrence, and drug resistance. Therefore, Wnt signal inhibitors should have the potency for the cancer treatment and prevention.[3,4] In the course of investigating new cancer prevention and treatment agents,[5,6] we also study new Wnt signal inhibitors from naturally occurring compounds. Herein, we isolated a Wnt signal inhibitor from the stems and twigs of *Lindera umbellata* Thunb. (Lauraceae). *L. umbellata* is a deciduous shrub that grows in the mountainous regions of Japan. The extract of this plant has long been used in Japan as a traditional medicine for the treatment of several gastrointestinal diseases. Essential oil has been reported to inhibit lipopolysaccharide-induced inflammation in RAW 264.7 cells.[7] Previous studies have described the chemical structures of constituents such as flavonoids,[8] chalcones, lignans,[9] and benzofuran derivatives.[10] Among them, the chalcones have various chemical structures via attaching with several monoterpenoids. Therefore, we pursued the isolation of these chalcones and related compounds from *L. umbellata*. This report deals with the structural elucidation of linderapyrone (**1**) and *epi*-(-)-linderol A (**2**), chemical synthesis of **1** and its related compounds from piperitone. Their inhibitory effects against Wnt signaling were evaluated as TCF/β-catenin transcriptional activity using a cell-based luciferase assay system.

The methanol extract of the stems and twigs of *L. umbellata* was partitioned in ethyl acetate–H_2O (1:1, v/v) to furnish an ethyl acetate-soluble fraction and aqueous layer. The ethyl acetate-soluble fraction was subjected to normal- and reversed-phase silica gel column chromatography and repeated high-performance liquid chromatography (HPLC) to give two new compounds linderapyrone (**1**) and *epi*-(-)-linderol A (**2**).

Linderapyrone (**1**, Fig. 1) was isolated as a yellowish gum with negative optical rotation ($[\alpha]^{25}_{D}$ −18.3 in MeOH). In the EI-MS of **1**, a molecular ion peak $[M]^+$ was observed at *m/z* 350 and the molecular formula $C_{23}H_{26}O_3$ was determined by HRMS measurement of the molecular ion peak. The ^{1}H NMR ($CDCl_3$) and ^{13}C NMR (Table 1) spectra of **1**, which were assigned by various NMR, showed signals assignable to the tri-substituted pyrone group [δ_H 6.12 (s, H-2)], an olefin group [δ_H 6.63 (d, J = 15.8 Hz, H-7), 7.38 (d, J = 15.8 Hz, H-8)], a phenyl group, and a monoterpene moiety {three methyl groups [δ_H 1.49 (s, H-7′), 0.78 (d, J = 6.2 Hz, H-9′), and 1.20 (d, J = 6.2 Hz, H-10′)], three methylene groups [δ_H 1.77 (m, H-2′ α), 1.82 (m, H-2′ β), 1.74 (m, H-5′ α), 1.11 (m, H-5′ β),1.62 (m, H-6′ α), and 2.10 (m, H-6′ β)], three methine groups [δ_H

* Corresponding authors.
E-mail addresses: tmatsumo@mb.kyoto-phu.ac.jp (T. Matsumoto), watanabe@mb.kyoto-phu.ac.jp (T. Watanabe).

https://doi.org/10.1016/j.bmcl.2021.128161
Received 26 March 2021; Received in revised form 6 May 2021; Accepted 25 May 2021
Available online 29 May 2021

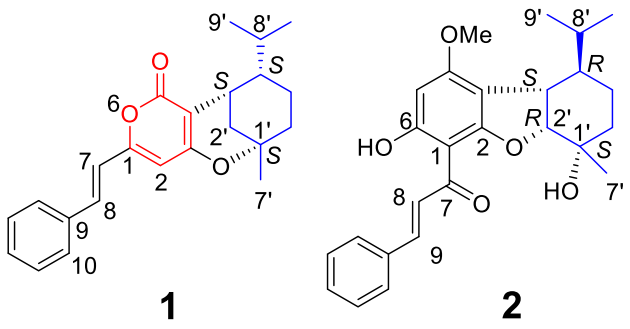

Fig. 1. Chemical structures of isolated compounds from *L. umbellata*.

Table 1
^{13}C NMR (150 MHz) and ^{1}H NMR (600 MHz) Spectroscopic Data ($CDCl_3$) for **1** and **2**.

Position	**1**		**2**	
	δ_C	δ_H (*J* in Hz)	δ_C	δ_H (*J* in Hz)
1	156.6		103.4	
2	112.3	6.12 (s)	161.0	
3	179.8		113.6	
4	100.4		161.7	
5	165.1		93.2	6.10 (m)
7	119.1	6.63 (d, *J* = 15.8)	166.6	
8	135.2	7.38 (d, *J* = 15.8)	191.2	
9	134.6		143.5	7.84 (d, *J* = 15.8)
10 and 14	127.3	7.50 (d, *J* = 7.6)	125.7	7.06 (d, *J* = 15.8)
11 and 13	128.9	7.39 (t, *J* = 7.6)	135.2	
12	129.4	7.38 (t, *J* = 7.6)	129.1	7.61 (d, *J* = 6.8)
13			128.4	7.42 (t, *J* = 6.8)
14			130.4	7.40 (t, *J* = 6.8)
15			128.4	7.42 (t, *J* = 6.8)
1′	82.7		129.1	7.61 (d, *J* = 6.8)
2′	37.2	α1.77 (m) β 1.82 (m)	70.7	
3′	27.4	3.54 (br-s)	92.8	4.37 (d, *J* = 5.5)
4′	49.2	1.26 (m)	41.0	3.02 (dd, *J* = 5.5, 11.0)
5′	22.3	α1.74 (m) β1.11 (m)	46.5	1.17 (m)
6′	39.1	α 1.62 (m) β2.10 (m)	20.4	α 1.62 (m) β 1.16 (m)
7′	27.8	1.49 (s)	36.1	α 1.79 (m) β 1.85 (m)
8′	30.0	1.25 (m)	25.1	1.35 (s)
9′	20.6	0.78 (d, *J* = 6.2)	27.0	1.87 (m)
10′	22.5	1.20 (d, *J* = 6.2)	15.3	0.88 (d, *J* = 6.8)

3.54 (br-s, H-3′), 1.26 (m, H-4′), and 1.25 (m, H-8′)], and a quaternary carbon bearing oxygen function [δ_C 82.7 (C-1′)]}. The connection of each moiety of **1** was confirmed based on DQF COSY and HMBC spectroscopy (Fig. 2). Namely, HMBC correlations were observed between H-2/C-1,4,7, H-8/C-9,10, H-3′/C-4,5,1′,5′, H-7′/C-1′,2′,6′, H-9′/C-4′,8′, and H-10′/C-4′,8′. The relative configuration of **1** was determined as (1′*S**,3′*S**,4′*S**) via analysis of their nuclear Overhauser effect spectroscopy (NOESY) spectra (Fig. 2). The NOESY cross-peaks of H-3′/H-4′ indicated that H-3′ and H-4′ are on one side. In addition, in the process of chemical synthesis of **1**, the intermediate **1c** that have same relative configuration as **1** was obtained less amount than diastereomer **1b** (Scheme 1). This result should be due to steric crowding and suggested that the H-3′ and H-4′ are on one side. CH_3-7′ and H-3′ are on one side because another configuration is impossible to exist based on its molecular strain. The absolute configurations of **1** were defined via comparison of the experimental and calculated electronic circular dichroism (ECD) data using the time-dependent density functional theory (TDDFT) method (Fig. 2).[11–13] Thus, the (1′*S*,3′*S*,4′*S*) absolute configurations of **1** was defined. Based on all this evidence, the chemical structure of **1** was determined as the unique pyrone derivative (Fig. 1).

Epi-(-)-linderol A (**2**, Fig. 1) was isolated as a yellowish gum with negative optical rotation ($[\alpha]^{25}_D$ −19.6 in MeOH). In the EI-MS of **2**, a molecular ion peak $[M]^+$ was observed at *m/z* 422 and the molecular formula $C_{26}H_{30}O_5$ was determined by HRMS measurement of the molecular ion peak. From the ^{1}H and ^{13}C NMR spectra of **2**, the overall structure was determined to be the same as (-)-linderol A,[14] except for the relative configurations of the monoterpene moiety. NOESY correlations were observed between H-2′/H-3′, H-3′/H-8′, and H-7′/H-2′ indicating that H-2′, H-3′, CH_3-7′, and CH-8′ are all on the same side. Therefore, the relative configuration of **2** was determined to be (1*S**,2*R**,3*S**,4*R**). The absolute configurations of **2** were defined as 1*S*,2*R*,3*S*,4*R* via comparison of the experimental and calculated ECD data using the TDDFT method (Fig. 2).[11–13] This optically pure compound was first isolated as a natural product in this study, but racemic it was previously reported as a synthetic intermediate by Dr. Yamashita *et. al.* (data not shown).[14] Mercifully, Dr. Yamashita provided us ^{1}H and ^{13}C NMR spectra of *epi*-linderol A and they were corresponded with that of **2** recorded in this study. Based on all this evidence, the chemical structure of **2** was determined to be *epi*-(-)-linderol A (Figure 1).

The inhibitory effects of **1** and **2** against TCF/*β*-catenin transcriptional activity (TOP activity) were evaluated using STF/293 cells. The cells were 293 human embryonic kidney cells stably transfected with modified M50 Super 8 × TOPFlash [luciferase reporter plasmid containing downstream of the TCF-binding site] with hygromycin resistant gene obtained from pGL4.32 vector as reported.[15] In this assay, the inhibitory effects of the test samples were assessed by observing the decrease in luciferase activity.[16,17] It was observed that **1** exerted a significant inhibitory effect without cytotoxicity. The chemical structure of **1** was completely different from previous reported Wnt signal inhibitors such as ICG-001 and IWR-1. Interestingly, **2** with chalcone and monoterpene moieties did not show an inhibitory effect (Fig. 3). Therefore, it is suggested that the pyrone moiety is necessary for inhibition of TOP activity.

Next, to evaluate the inhibitory effects on TOP activity and the mechanism of **1** and its related compounds, we synthesized **1** from piperitone (**1a**) according to a previous report (Scheme 1).[18] Briefly, catalytic reduction of **1a** yielded piperitol (**1b**). Through acid-promoted S_N1 substitution and intramolecular etherification, **1c** (minor product) and **1d** (major product) were obtained from **1b**. Finally, **1c** was treated with *n*-BuLi at −78 °C and benzaldehyde to obtain a reaction intermediate that was treated with Ac_2O/TEA followed by the addition of DBU obtained **(±)-1** (mixture of **1** and its enantiomer). HPLC separation using a chiral column successfully produced optically pure **1** and its enantiomer (***ent*-1**). Using the same reaction, **1da** (racemic mixture) was synthesized from **1d**. In addition, 4-methoxy-6-methylpyrone (**1e**) and 5,6-degydrokawain (**1f**) was easily synthesized for structure–activity relationship stud-ies.[19,20]

The inhibitory effects against TOP activity of the piperitone (**1a**), synthetic intermediates (**1c** and **1d**), and related compounds (*ent*-**1**, **1d**, **1e**, and **1f**) were evaluated. The enantiomer (*ent*-**1**) and diastereomer (**1da**) showed significant inhibitory effects, and their effects were equivalent to those of natural product **1** (Fig. 3). Monoterpene (**1a**) and pyrones (**1e** and **1f**) did not display inhibitory effects. In contrast, synthetic intermediates **1c** and **1d** having both moieties showed weak effects (Supporting Information). According to these data, some structure-activity relationships were suggested. Namely, the stereochemistry of the monoterpene moiety is not limited as a naturally occurring compound for inhibitory effects against TOP activity. Both the monoterpene and pyrone moiety are necessary, and the phenyl group at C-8 may contribute to the enhancement of these effects.

The inhibitory effects against TOP activity of **1**, ***ent*-1**, and **1da** were confirmed by the cell viability on HT-29 human colon cancer cell. Wnt signaling pathway contributes to HT-29 cell proliferation.[21] The viability of HT-29 cells was significantly decreased by **1**, **±1**, and **1da** treatment for 72 hr (Fig. 4) and 24 hr (Supporting Information). The IC50 values of **1** (IC50: 32.4 ± 2.3) and **±1** (IC50: 19.9 ± 7.6) were not stronger than those of positive control ICG-001 (IC50: 10.8 ± 2.0) and

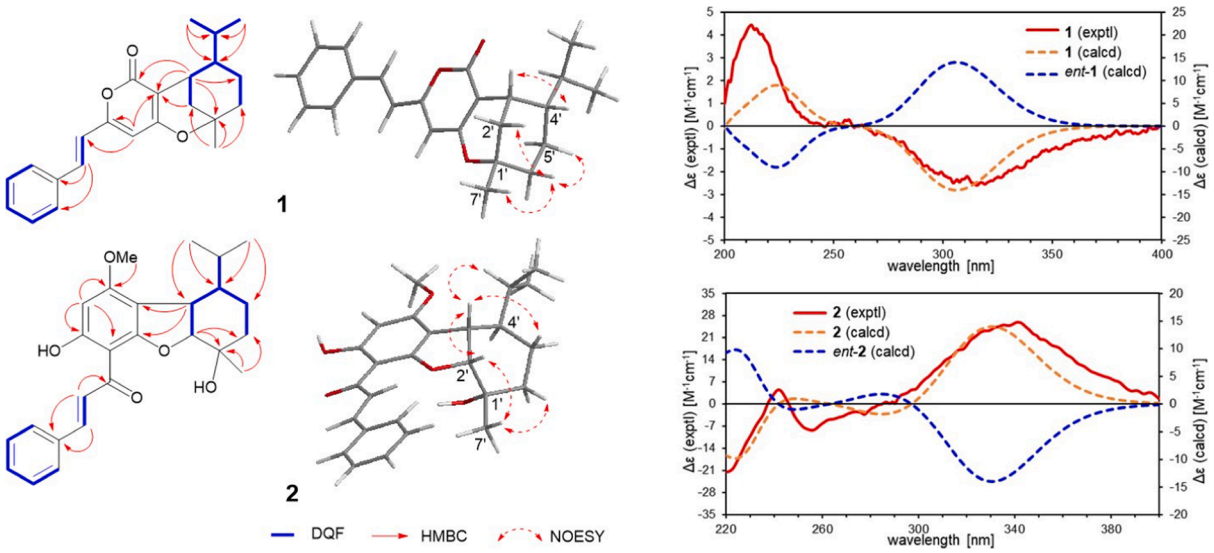

Fig. 2. Key 2D NMR spectra of new compounds (**1** and **2**) and ECD spectra of **1** and **2**.

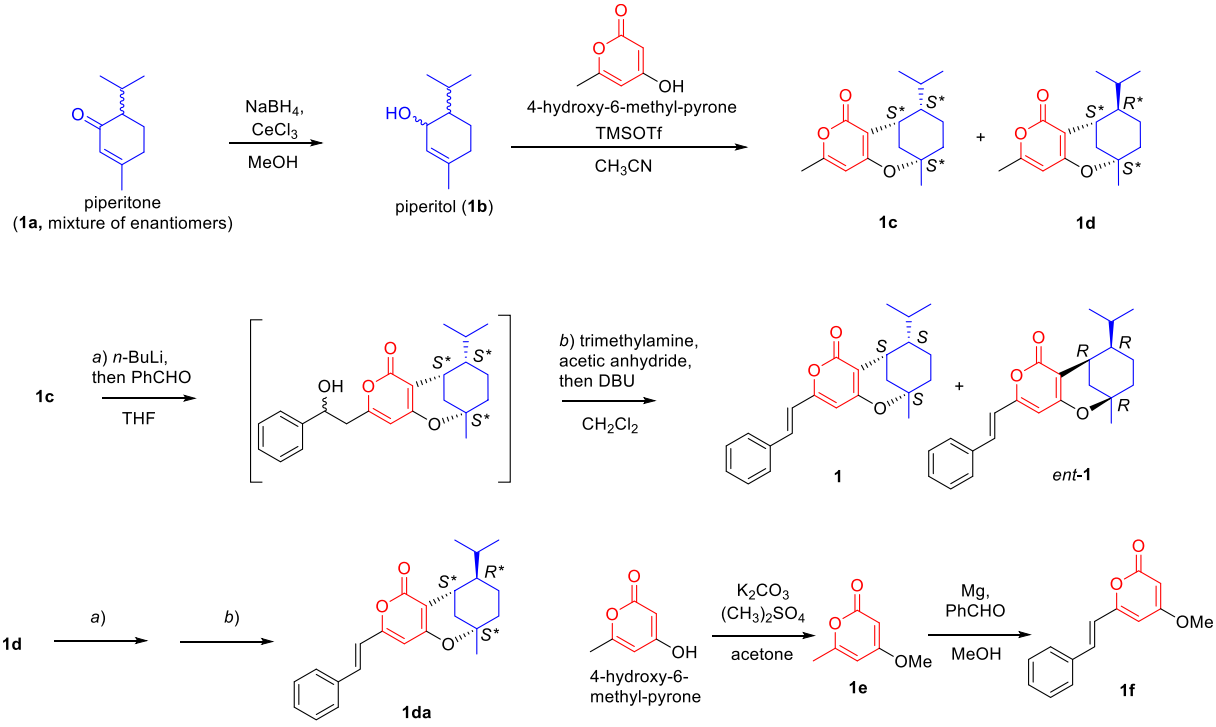

Scheme 1. Synthesis of **1** and Related Compounds (**1b–1f**, *ent*-**1**, and **1da**).

IWR-1 (IC50: 9.52 ± 1.2). In contrast, **1da** (IC50: 8.2 ± 2.3) exhibited cytotoxicity at lower concentrations than the positive control.

To evaluate the mechanism of the inhibitory effect against TOP activity of **1da**, we evaluated the alteration of gene expression of **1da**-treated HT-29 cells by cDNA microarray analysis. The results demonstrated that 122 mRNAs were upregulated (ratio ≥ 2.00) and 152 mRNAs were downregulated (ratio ≤ 0.50) compared with control group by 5 μM **1da** treatment for 24 hr (supporting information). Pathway analysis using Gene-Spring GX software (Tomy Digital Biology, Tokyo, Japan) with downregulated genes suggested that **1da** may affects two Wnt-related signaling pathways (Fig. 5, red bars) together with other signals. Especially, several genes, which are regulated by small-molecule compounds in Wnt-*β*-catenin signaling, were decreased by **1da** treatment. Among **1da**-downregulated genes, TCF-4 is the key transcription factor which activates as complex with β -catenin in Wnt signaling pathway.[3,4] Therefore, **1da** may inhibit Wnt signaling pathway via downregulation of the expression level of TCF-4.

According to the above results, we modified the chemical structure of **1da** to obtain a stronger Wnt signal inhibitor. We synthesized derivatives **1db**–**1dg** from **1d** using several aldehydes. Catalytic reduction of **1da** yielded **1dh** which lacked double bond in the side chain Fig. 6A.[22] The inhibitory effect of **1dg** against TOP activity was much stronger than that of ICG-001 because it showed lower cytotoxicity in the luciferase assay system Fig. 6B. In addition, **1dg** showed strong anti-proliferation effect same as the inhibitory effect against TOP activity. Therefore, we concluded **1dg** is the strongest Wnt signaling inhibitor in this paper. On the other hand, **1db** showed strongest anti-proliferation effect among all compounds, but the inhibitory effect against TOP

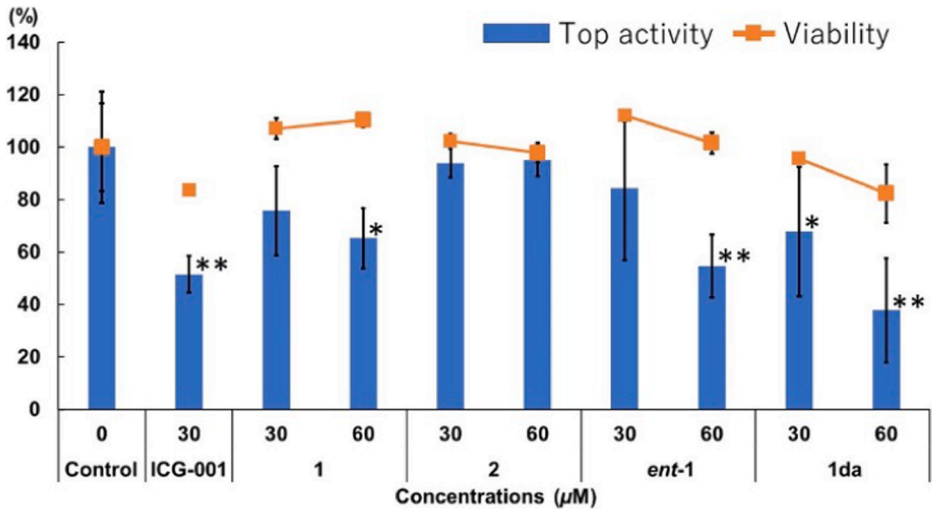

Fig. 3. The inhibitory effects against TOP activity and the cell viability for **1, 2**, *ent*-**1**, and **1da**.

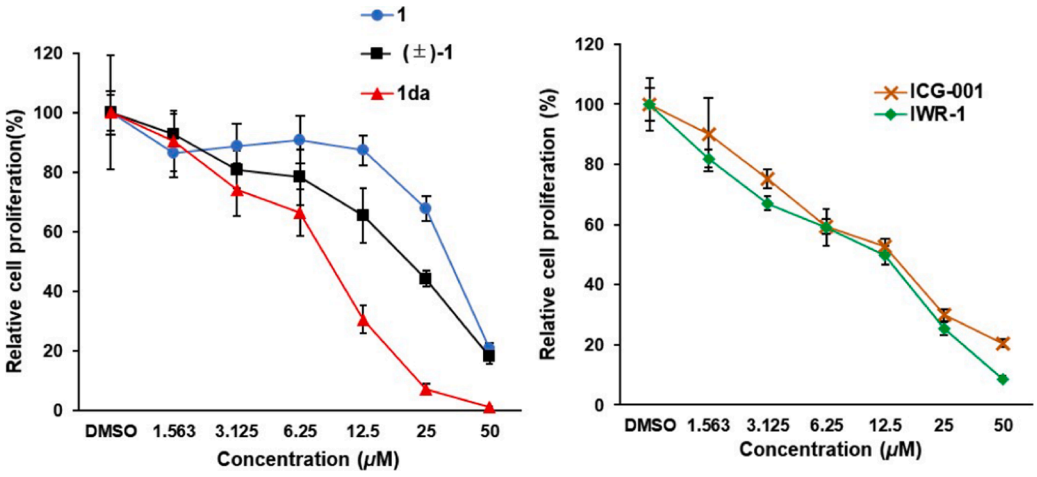

Figure 4. The cell viability of **1**, ±**1**, **1da**, and positive controls on HT-29 cell.

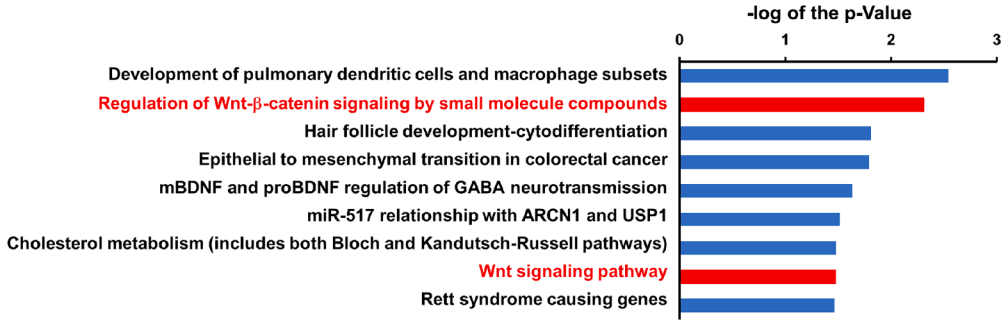

Fig. 5. Pathway analysis of differentially regulated genes in **1da**-treated HT-29 cells compared with DMSO-treated groups. The 152 genes identified as down-regulated (ratio ≤ 0.50) were subjected to pathway analysis. The 9 regulated pathways at the $P < 0.05$ level are presented as -log of the p-Values.

activity was weaker than **1dg**. Therefore, **1db** may inhibited not only Wnt signaling pathway but also other pathways Fig. 6C.

In conclusion, **1** isolated from *L. umbellata* and its derivatives were synthesized in short steps. The inhibitory effects of **1**, ***ent*-1**, and **1da** against Wnt signaling was evaluated using the luciferase assay system, cell viability, and pathway analysis. Moreover, we synthesized a derivative (**1dg**) that has a stronger inhibitory effect than the positive control and **1**. Therefore, it is possible that **1** is a novel lead compound which can act as a Wnt signal inhibitor. Further studies of **1** such as determination of target protein and further chemical structure derivatization may provide us new cancer treatment drug.

Declaration of Competing Interest

The authors declare that they have no known competing financial interests or personal relationships that could have appeared to influence

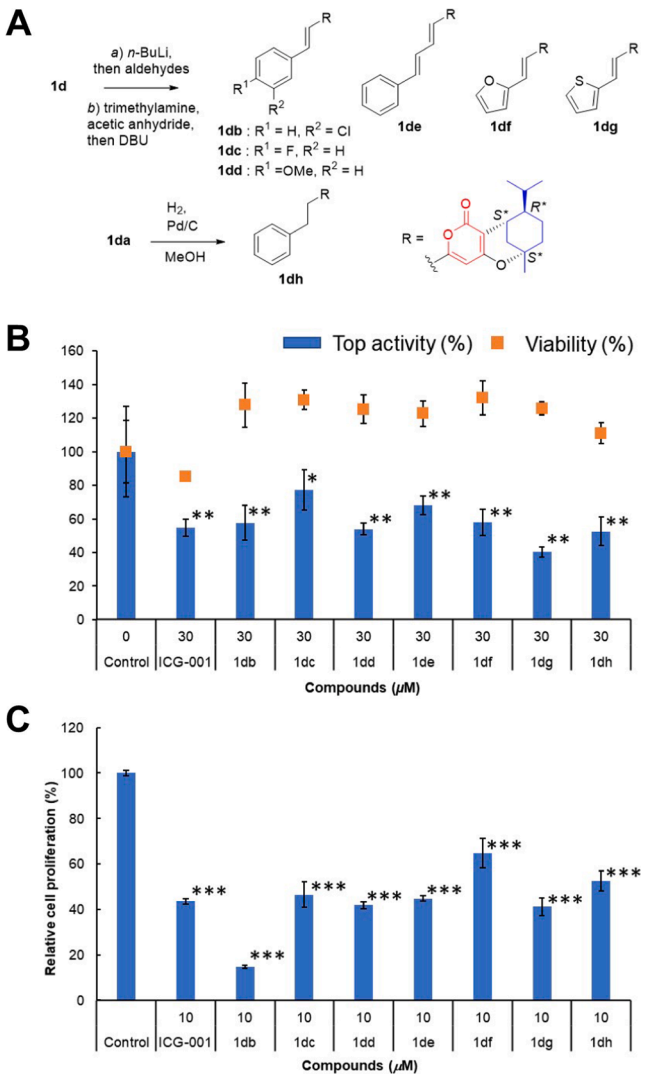

Fig. 6. (**A**) Synthesis of **1d** derivatives (**1db**–**1dh**). (**B**) Their inhibitory effects against TOP activity. (**C**) Their inhibitory effects against relative cell proliferation on HT-29 cells.

the work reported in this paper.

Acknowledgements

This work was supported by JSPS KAKENHI (Grant Number 20H03397 and 20J14567). We thank Dr. Yamashita (Kyoto Pharmaceutical University) for provided us ^{1}H and ^{13}C NMR spectra of *epi*-linderol A.

Appendix A. Supplementary data

Supplementary data to this article can be found online at https://doi.org/10.1016/j.bmcl.2021.128161.

References

1 Sato T, Arai M, Yixizhuoma, et al. Cadinane sesquiterpe-noids isolated from Santalum album using a screening program for Wnt signal inhibitory activity. *J Nat Med*. 2020;74:476–481.
2 Ishibashi M. Screening for natural products that affect Wnt signaling activity. *J Nat Med*. 2019;73:697–705.
3 Ashihara E, Takada T, Maekawa T. Targeting the canonical Wnt /β-catenin pathway in hematological malignan-cies. *Cancer Sci*. 2015;106:665–671.
4 Yao H, Ashihara E, Maekawa T. Targeting the Wnt/β -catenin pathway in human cancers. *Expert Opin Ther Target*. 2011;15:873–887.
5 Matsumoto T, Imahori D, Achiwa K, et al. Chemical structures and cytotoxic activities of the constituents isolated from Hibiscus tiliaceus. *Fitoterapia*. 2020;142:104524. https://doi.org/10.1016/j.fitote.2020.104524.
6 Matsumoto T, Imahori D, Saito Y, et al. Cytotoxic activities of sesquiterpenoids from the aerial parts of *Petasites japonicus* against cancer stem cells. *J Nat Med*. 2019;74:689–701.
7 Maeda H, Yamazaki M, Katagata Y. Kuromoji (*Lindera umbellata*) essential oil inhibits LPS-induced inflammation in RAW 264.7 cells. *Biosci Biotechnol Biochem*. 2013;77:482–486.
8 Ichino K, Tanaka H, Ito K. A new flavanone, neolindera-tone, from *Lindera umbellata* THUNB. Var. lancea MOMIYAMA. *Chem Pharm Bull*. 1989;37:1426–1427.
9 Kuroda M, Sakurai K, Mimaki Y. Chemical constituents of the stems and twigs of *Lindera umbellata*. *J Nat Med*. 2011;65:198–201.
10 Mimaki Y, Kameyama A, Sashida Y, Miyata Y, Fujii A. A novel hexahydrodibenzofuran derivative with potent inhibitory activity on melanin biosynthesis of cultured B-16 melanoma cells from *Lindera umbellata* bark. *Chem Pharm Bull*. 1995;43:893–895.
11 Pescitelli G, Bruhn T. Good computational practice in the assignment of absolute configurations by TDDFT calculations of ECD spectra. *Chirality*. 2016;28(6):466–474.
12 Gaussian 09, A.01 ed. Wallingford, C.T: Gaussian Inc; 2009.
13 Bruhn T, Schaumlöffel A, Hemberger Y, Bringmann G. SpecDis: Quantifying the comparison of calculated and experimental electronic circular dichroism spectra. *Chirality*. 2013;25:243–249.
14 Yamashita M, Shimizu T, Kawasaki I, Ohta S. Determination of the absolute configuration and the first total synthesis of (-)-and (+)-linderol A. *Tetrahedron Asymm*. 2004;15:2315–2317.
15 Wakabayashi R, Hattori Y, Hosogi S, Toda Y, Ashihara E. A novel dipeptide type inhibitor of the Wnt/ β -catenin pathway suppresses proliferation of acute myelogenous leukemia cells. *Biochem Biophys Res Commun*. 2020;535:73–79.
16 Shono T, Ishikawa N, Toume K, et al. Cerasoidine, a bis-aporphine alkaloid isolated from *Polyalthia cerasoides* during screening for Wnt signal inhibitors. *J Nat Prod*. 2016;79:2083–2088.
17 Bae ES, Kim YM, Kim DH, et al. Anti-proliferative activity of nodosin, a diterpenoid from *Isodon serra*, via regulation of Wnt/β-catenin signaling pathways in human colon cancer cells. *Biomol Ther*. 2020;28:465–472.
18 Zhang P, Wang Y, Bao R, Luo T, Yang Z, Tang Y. Enantioselective biomimetic total synthesis of katsumadain and katsumadain C. *Org Lett*. 2012;14:162–165.
19 Rizzo A, Trauner D. Toward (−)-enterocin: an improved cuprate barbier protocol to overcome strain and sterical hindrance. *Org Lett*. 2018;20:1841–1844.
20 Li C, Cheng B, Fang S, Zhou H, Gu Q, Xu J. Design, syntheses and lipid accumulation inhibitory activities of novel resveratrol mimics. *Eur J Med Chem*. 2018;143:114–122.
21 Ghanavati R, Akbari A, Mohammadi F, et al. Lactobacillus species inhibitory effect on colorectal cancer progression through modulating the Wnt/β-catenin signalling pathway. *Mol Cell Biochem*. 2020;470:1–13.
22 Dethe DH, Dherange BD. Enantioselective total syntheses of (+)-hostmanin A, (−)-linderol A, (+)-methyllinderatin and structural reassignment of aduncin E. *J Org Chem*. 2015;80:4526–11531.